Electromechanical Impedance Spectroscopy and Guided Wave Propagation Predictive Modeling on Composite Materials

Matthieu Gresil, Victor Giurgiutiu

7th European Workshop on Structural Health Monitoring
July 8-11, 2014. La Cité, Nantes, France

ELECTROMECHANICAL IMPEDANCE SPECTROSCOPY AND GUIDED WAVES PROPAGATION MODELLING ON COMPOSITE MATERIALS

Matthieu Gresil[1], Victor Giurgiutiu[2]

[1] *School of Materials, University of Manchester, Paper Science Building, 79 Sackville Street, Manchester, M13 9PL, UK.*
[2] *LAMSS, Department of Mechanical Engineering, University of South Carolina, 300 Main Street, Columbia SC, 29208, USA.*

matthieu.gresil@manchester.ac.uk

ABSTRACT

Electromechanical impedance spectroscopy (EMIS) and guided wave (GUW) propagation are a popular structural health monitoring (SHM) technique, which had found applications in many fields of engineering: mechanical, aerospace, civil and others. Piezoelectric wafer active sensors (PWAS) are lightweight and inexpensive transducers that enable a large class of SHM applications such as: (a) embedded GUW ultrasonic, i.e., pitch-catch, pulse-echo, phased arrays; (b) high-frequency modal sensing, i.e., EMIS method; and (c) passive detection, i.e., acoustic emission (AE).
The aim of the work presented in this paper is to provide tools to extend modelling capacities and improve quality and reliability of EMIS and 2-D GUW propagation models using commercially available multi-physics finite element method (MP-FEM) packages on fibre reinforces polymers (FRP). The focus of this paper is on the challenges posed by using PWAS transducers in the composite laminate structures as different from the metallic structures on which this methodology was initially developed.

KEYWORDS : *Composite materials, piezoelectric wafer active sensors, electromechanical impedance, guided waves, multi-physics finite element method.*

INTRODUCTION

Electromechanical impedance spectroscopy (EMIS) and guided waves (GUW) using piezoelectric wafer active sensors (PWAS) have been shown as an effective structural health monitoring (SHM) techniques, and have useful applications in various fields of engineering: mechanical, aerospace, civil, and others [1].
Over the past decade, substantial efforts have been devoted to the analytical and numerical modelling of various aspects of the EMIS method [2-4]. However, the majority of prior studies are focused on fundamental understanding of the sensor transduction mechanism and sensor-structure interaction. Analytical models are often unsuitable for practical applications because they only consider simple structures such as beams, plates and shells with easy to simulate boundary conditions. More importantly, most of the previous work is on isotropic (such as metallic) or heterogeneous (such as concrete) structures. EMIS applications to orthotropic laminated composites have also been studied and discussed in literature to a lesser extent [5-7]. Subsequent developments in various numerical methods, such as the finite element method (FEM), were found to be an ideal alternative [8, 9].
In parallel, GUW are ultrasonic waves which propagate through plate-like structures and are employed for SHM applications. GUW features used for SHM are time-of-flight, mode conversion/generation, change in amplitude/attenuation, velocity, etc. [1]. Attenuation is often neglected in wave propagation analysis because of modelling complexities. In the case of fibre

reinforced polymer (FRP), one of the main complexities involved in the propagation of guided waves is the attenuation effect. The different sources of energy dissipation in FRP are: (a) viscoelastic nature of matrix and/or fibre materials [10] ; (b) damping due to interphase [11]; (c) damping due to damage [12] ; (d) visco-plastic damping [13]. (e) thermo-elastic damping [13]. Numerical modelling of guided wave propagation helps understanding the interaction between the material damage and the guided waves.

This paper presents multi-physics finite element modelling (MP-FEM) of PWAS EMIS and GW for SHM applications on FRP structures. The MP-FEM implementation allows for the consideration of the contributions of the active material, the adhesive bond and the structural damage. Numerical studies show good correlation with experimental results with appropriate level of structural damping. The proportionality damping constants are shown to depend on the attenuation coefficient, group velocity, and central frequency of excitation.

After a brief introduction, the paper reviews the PWAS-based SHM principles. It follows with a discussion of EMIS and GUW propagation in composites. Experiments were performed on a FRP laminate, employing PWAS to measure the attenuation coefficient. Finally, the paper presents some experimental and MP-FEM results on EMIS and GUW propagation in composite laminate specimens.

1 ELECTROMECHANICAL IMPEDANCE SPECTROSCOPY

PWAS can be used as active sensing devices that provide bidirectional energy transduction from the electronics into the structure, and also from the structure back into the electronics. PWAS can be used as collocated electromechanical impedance sensor-actuators that permit effective modal identification in a wide frequency band [14-17]. In an embedded sensing system, the PWAS can be embedded into the structures by mounting them directly onto the structure and then leaving them in place to perform their structural health-monitoring task (such a thing would be unthinkable with conventional ultrasonic transducers, which are bulky, obtrusive, and expensive).

1.1 The PWAS electromechanical impedance method

For a linear piezoelectric material, the relation between the electrical and the mechanical variables can be described by linear relations:

$$\begin{bmatrix} S \\ D \end{bmatrix} = \begin{bmatrix} s^E & d_t \\ d & \varepsilon^T \end{bmatrix} \begin{bmatrix} T \\ E \end{bmatrix} \tag{1}$$

where S is the mechanical strain; T is the mechanical stress; E is the electric field; D is the charge density; s is the mechanical compliance; d is the piezoelectric strain constant; and ε is the permittivity. The superscripts E and T indicate that those quantities are measured with electrodes connected together and zero stress, respectively, and the subscript t indicates transpose. The first equation describes the converse piezoelectric effect and the second describes the direct effect.

The principles of electromechanical impedance method are illustrated in Figure 1. The drive-point impedance presented by the structure to the active sensor can be expressed as the frequency dependent variable $Z_{str}(\omega) = k_{str}(\omega)/j\omega = k_e(\omega) - \omega_m^2(\omega) + j\omega c_e(\omega)$. Through the mechanical coupling between PWAS and the host structure, on one hand, and through the E/M transduction inside the PWAS, on the other hand, the drive-point structural impedance is reflected directly in the electrical impedance, $Z(\omega)$, at the PWAS terminals

$$Z(\omega) = \left[j\omega c \left(1 - \kappa_{31}^2 \frac{\chi(\omega)}{1+\chi(\omega)} \right) \right]^{-1} \tag{2}$$

where C is the zero-load capacitance of the PWAS and κ_{31} is the E/M cross coupling coefficient of the PWAS $\left(\kappa_{31} = d_{31} \Big/ \sqrt{\bar{s}_{11}\bar{\varepsilon}_{33}}\right)$, and $\chi(\omega) = k_{str} / k_{PWAS}$ with k_{PWAS} being the static stiffness of the PWAS.

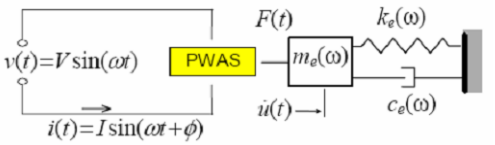

Figure 1 : Electromechanical coupling between PWAS and structure for an 1-D dynamic model

1.2 PWAS EMIS experimental measurement

The electromechanical impedance SHM method is direct and easy to implement, the only required equipment being an electrical impedance analyser, such as the HP 4192A impedance analyser. An example of performing PWAS electromechanical impedance spectroscopy is presented in Figure 2. The HP 4194A impedance analyser (Figure 2a) reads the in-situ electromechanical impedance of the PWAS attached to a specimen. It is applied by scanning a predetermined frequency range in the high kHz band (up to 15 MHz) and recording the complex impedance spectrum.

(a)

(b)

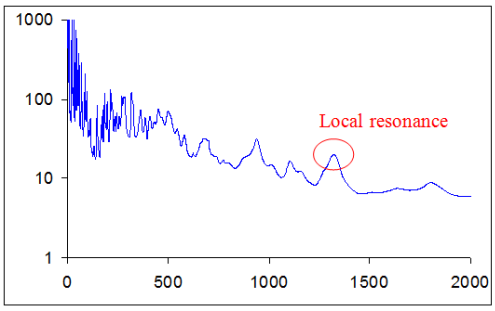

Figure 2: (a) Impedance analyser; (b) example of measured impedance spectrum.

During a frequency sweep, the real part of the E/M impedance, $\mathrm{Re}[Z(\omega)]$, follows the up and down variation as the structural impedance goes through the peaks and valleys of the structural resonances and anti-resonances (Figure 2b). By comparing the real part of the impedance spectra taken at various times during the service life of a structure, meaningful information can be extracted pertinent to structural degradation and ongoing damage development. On the other hand, analysis of the impedance spectrum supplies important information about the PWAS integrity. The frequency range used in the E/M impedance method must be high enough for the signal wavelength to be significantly smaller than the defect size. From this point of view, the high frequency EMIS method differs from the low-frequency modal analysis approaches.

1.3 3D MP-FEM EMIS modelling

In the MP-FEM approach, the mechanical coupling between the structure and the sensor is implemented by specifying boundary conditions of the sensor while the electromechanical coupling is modelled by multi-physics equations for the piezoelectric material. The first coupling allows the mechanical response sensed by the piezoelectric element to be reflected in its electric signature composite. The glass fibre reinforced polymer (GFRP) structure considered in this study is modelled as a homogeneous orthotropic material [8]. The test specimen is numerically modelled with the MP-FEM method using a 3D mesh. The SOLID186 layered structural solid element is used to model the five layers laminated GFRP composite specimen with layer orientation of 0 degree on the x-axis; the adhesive layer is modelled with the SOLID95 element. The PWAS transducer is modelled with the SOLID226 coupled field element. Each element has twenty nodes. At low

frequency (below 500 kHz), at medium frequency (500 kHz to 5 MHz) and at high frequency (5 to 15 MHz), the size of the mesh is 1mm, 0.5mm and 0.1mm respectively, to obtain a good convergence of the problem.
The comparison between the simulated and the experimental impedance spectra results are presented in Figure 3. In Figure 3a, the results are in the range up to 5 MHz. It is apparent that a relatively good agreement between the experiments and 3D MP-FEM simulation has been achieved. The good matching is achieved by adjusting the damping coefficients used in the structural model. The correlation of the modal frequencies between the experimental and the numerical results is quite good, especially at higher frequencies. However, some discrepancies in the magnitudes of some resonances are observed, especially in the range of 450 to 650 kHz. It is interesting to see that the best match is obtained in the 700 kHz to 2 MHz frequency range. This is very beneficial, because this frequency range has shown the best detection of delamination damage [8].

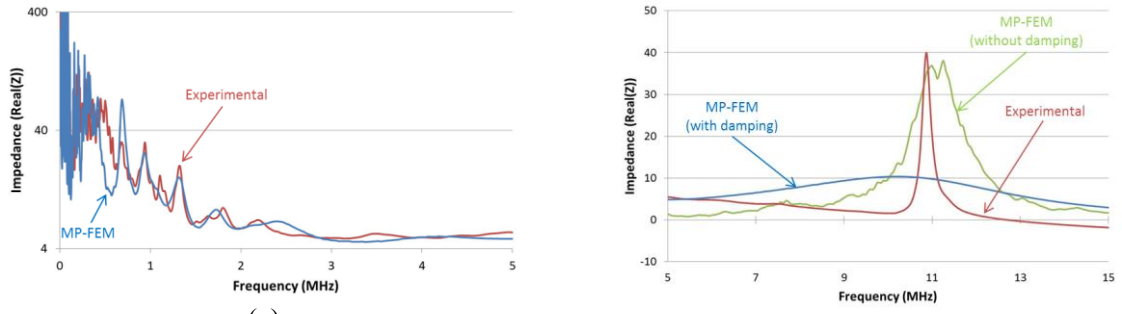

Figure 3 : Comparison of experimental and 3D MP-FEM model impedances spectra of laminate GFRP (a) for a frequency range 10 kHz to 5 MHz; (b) for a frequency range 5 MHz to 15 MHz.

Figure 3b shows a comparison of the impedance spectra in a very high frequency range (of 5 to 15 MHz). Only one peak is observed at ~11 MHz; this peak corresponds to the thickness mode resonance of the PWAS transducer. It seems that at high frequency (5 to 15 MHz), the vibration is localized near the PWAS so the bonding condition and the PWAS geometry is very important. In the case of the simulation the bonding layer is perfect and also the PWAS geometry. In reality, this is not true so we can explain more difference between the experimental and the simulation results for high frequency. Moreover the magnitude of the vibration pick is very small due to the damping effect, and this effect is very hard to simulate because of the non-linearity of this effect.
The comparison between the 3D simulation and experimental results has revealed two different regions of behaviour: (1) below 5 MHz, the experimental result matches the result from a 3D model with structural damping (Figure 3a); (2) however, above 7 MHz, the experimental result matches better with a 3D model without structural damping (Figure 3b). One possible explanation is that at lower frequency the vibration covers a larger area and the overall structural damping is important; whereas at high frequency the vibration is localized in thickness mode resulting that the structural damping has negligible effect. In comparison with other models of the EMIS technique, the model discussed here exhibits remarkable robustness at very high frequency.

1.4 Fibre orientation effect

For laminate composite material, the fibre orientation is very important for the mechanical behaviour of the structure. So we decided to study the EMIS for different fibre's orientation to know if the impedance spectra change with different orientation. The experimental results for two different fibre orientations (0 and 45 degree) in a high frequency range (10 kHz to 5 MHz) are presented in Figure 4a. It is apparent that a frequency shift to the lower frequency is present for the fibre orientation of 45 degree. Figure 4b shows the MP-FEM impedance spectra for these two different orientations. It is apparent that a frequency shift to the lower frequency is present for the layer orientation of 45 degree; this is in agreement with the experimental results.

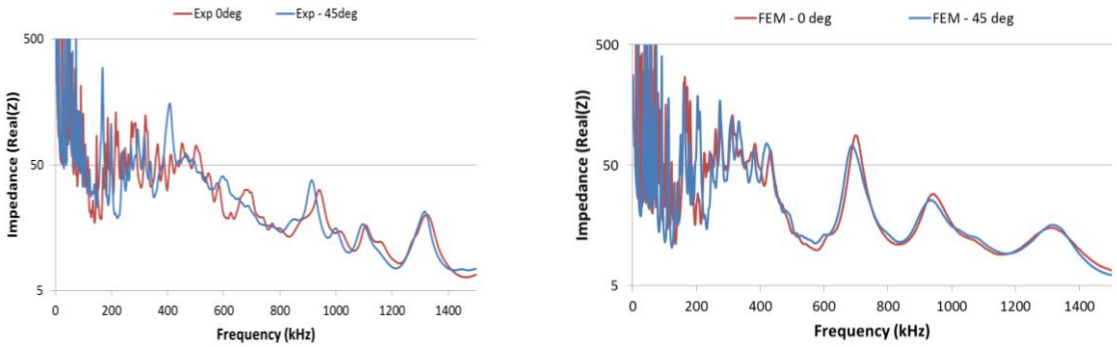

(a) (b)

Figure 4 : Fibre orientation effect on the impedance spectra; (a) Experimental results for 0 and 45 degree on the x-axis; (b) MP-FEM results for 0 and 45 degree on the x-axis.

2 GUIDED WAVE PROPAGATION IN COMPOSITES

2.1 Materials under test and experimental set-up

The structure under investigation is a CFRP plate consisting of a carbon-fibre fabric reinforcement in an epoxy resin (Figure 5). The plate dimensions are $390 \times 395 \times 2\,\text{mm}^3$. The CFRP material is HexPly® M18/1/939; this is a woven carbon prepreg manufactured by Hexcel. This material is commonly used in aircraft industry. The plate plies have the orientation $[0, 45, 45, 0]_s$. The CFRP material properties given by the manufacturer are presented in Table 1.

Table 1: CFRP mechanical properties from Hexcel

E_{11}	E_{22}	E_{33}	ν_{12}	ν_{13}	ν_{23}	G_{12}	G_{13}	G_{23}	ρ
65 GPa	67 GPa	8.6 GPa	0.09	0.09	0.3	5 GPa	5 GPa	5 GPa	1605 kg/m^3

Twenty one PWAS transducers (Steminc SM412, 8.7 mm-diameter disks and 0.5 mm-thick) were used for Lamb wave propagation experiments. The PWAS network bonded on the CFRP plate is shown on Figure 5. The instrumentation consisted of an HP33120A arbitrary signal generator, and a Tektronix TDS210 digital oscilloscope. A LabView™ computer program was developed to record the data from the digital oscilloscope, and to generate the raw data files.

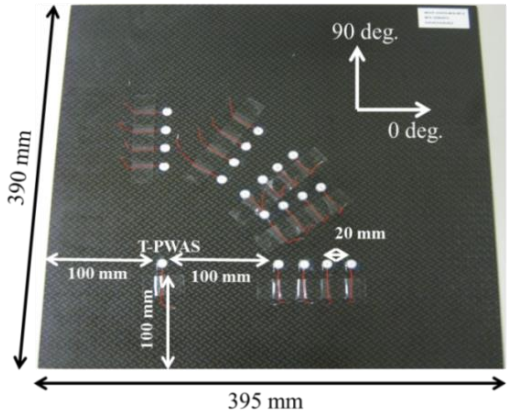

Figure 5 : Picture the network of piezoelectric wafer active sensor bonded on the CFRP.

2.2 Simulation of the GW propagation with Rayleigh damping

The MP-FEM simulation was carried out on a CFRP laminate described in the section 2.1 to determine the attenuation coefficient. A 150 kHz three-tone burst modulated by a Hanning window with a 20 Volts maximum amplitude peak to peak was applied to the top surface of the T-PWAS transducer, and the other PWAS transducers as receivers. Due to the dispersion curves presented and the tuning effect described on reference [18], both S0 and A0 modes are present at this frequency. Figure 6 shows the comparison between the MP-FEM simulation and experimental electric signal measured at R-PWAS placed at 100 mm from the T-PWAS with the stiffness proportional coefficient $\beta = 2.10^{-8}$ which corresponds to the A0 mode attenuation as calculated in the reference [19]. With this stiffness proportional coefficient $\beta = 2.10^{-8}$, the MP-FEM signal for the S0 and the A0 modes are in very good agreement with the experimental signal.

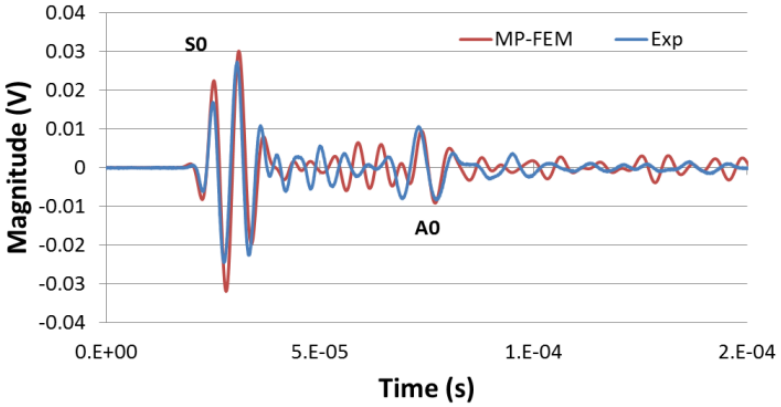

Figure 6 : Comparison between the experimental and the MP-FEM received signal at 100 mm from the T-PWAS at 150 kHz with $\alpha = 0$ and $\beta = 2.10^{-8}$.

However, the MP-FEM signal between the S0 mode packet and the A0 mode packet is different from the experimental signal. This different signal may be due to the scattering effect by the other bonded PWAS on the guided wave propagation path between the T-PWAS and the R-PWAS as described on the MP-FEM snapshot on Figure 7.

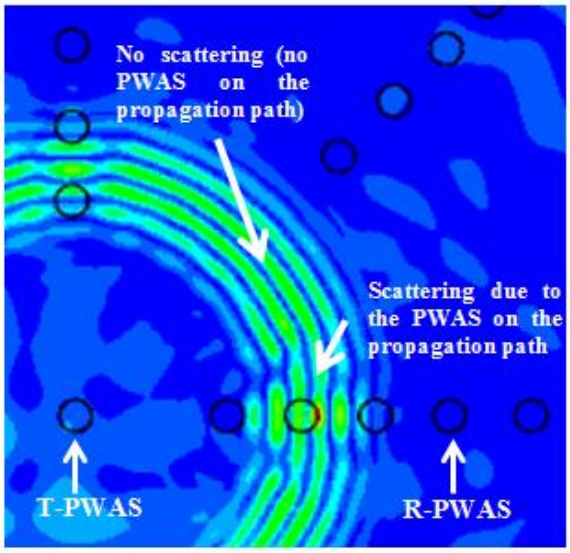

Figure 7 : Snapshot of the guided waves propagation showing the scattering due to the bonded PWAS on the guided wave propagation path between the T-PWAS and the R-PWAS.

In addition, we may attribute these phenomena to a micro defect that we observed in the structure as shown on the scanning acoustic microscopy picture on Figure 8a and Figure 8b. Indeed, on the first layer (0/90 degree) and on the second layer (45/-45 degree), we observe some area of resin pocket and lake of resin, respectively. These micro defects can create some scattering effect and/or conversion mode on the guided wave which is observed on the received signal on Figure 6.

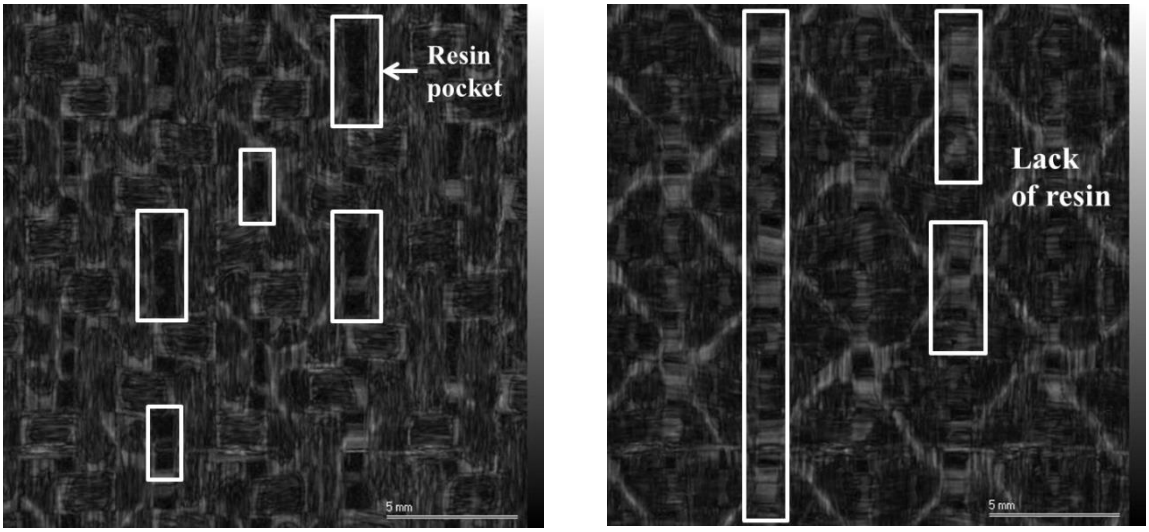

(a) (b)

Figure 8 : Scanning acoustic microscopy : a) first layer at 0/90 degree ; (b) second layer at 45/-45 degree

CONCLUSION

This paper has presented multi-physics finite element modelling of electromechanical impedance spectroscopy and guided waves using piezoelectric wafer active sensors for structural health monitoring applications on FRP structures.

The 3-D MP-FEM method was used to simulate realistic situations that were then compared with EMIS experimental results. The 3D MP-FEM model gave excellent reproduction of the measured EMIS results; however, the required computation is orders magnitude larger than the 2D MP-FEM. It was found that this numerical model exhibited remarkable robustness at a very high frequency. We also found that the structural damping is very important for proper modelling of the interaction between the host structure and the PWAS. At lower frequencies, the damping effect of the composite specimen is very important, because the vibration given by the PWAS has a global coverage over the whole structure; in contrast, at higher frequencies, the vibration in the structure is more localized near the PWAS and the structural damping does not play good role.

The Rayleigh damping model was used to compute the wave damping coefficient for S0 and A0 mode. The multi-modal guided wave propagation was examined by excitation at 150 kHz where both the A0 and S0 modes are present. Using the mass and stiffness coefficients, we were able to simulate these two modes using our MP-FEM approach with high accuracy.

Future work should continue the MP-FEM investigation in the effect of different types of defects (cracks, fibre break, delamination…) and comparison of these findings with experimental results consisting of EMIS and GW readings on specimens with internal damage and PWAS disbonds or damage.

ACKNOWLEDGMENTS

This work was supported by Office of Naval Research through the Naval International Cooperative Opportunities in Science and Technology Program (Grant no. N00014-09-1-0364; Program sponsor

Dr. Ignacio Perez). Dr. Nik Rajic from the Defence Science and Technology Organization is thankfully acknowledged for having provided the composite material. Dr. Sourav Banerjee from the University of South Carolina is thankfully acknowledged for the scanning acoustic microscopic pictures.

REFERENCES

1. Giurgiutiu, V., *Structural Health Monitoring With Piezoelectric Wafer Active Sensor*. 2008: Elsevier Academic Press.
2. Lim, Y.Y., S. Bhalla, and C.K. Soh, *Structural identification and damage diagnosis using self-sensing piezo-impedance transducers.* Smart Materials and Structures, 2006. **15**(4): p. 987-995.
3. Giurgiutiu, V., et al., *Predictive modeling of piezoelectric wafer active sensors interaction with high-frequency structural waves and vibration.* Acta Mechanica, 2012. **223**(8): p. 1681-1691.
4. Makkonen, T., et al., *Finite element simulations of thin film composite BAW resonators.* IEEE Transactions on Ultrasonics, 2001. **48**: p. 1241-1258.
5. Bois, C., P. Herzog, and C. Hochard, *Monitoring of delamination in laminated composite beam using in-situ measurments and parametric identification.* Journal of Sound and Vibration, 2007. **299**: p. 786-805.
6. Bois, C. and C. Hochard, *Monitoring of Laminated Composites Selamination Based on Electromechanical Impedance Measurment.* Journal of intelligent material systems and structure, 2004. **15**: p. 59-67.
7. Yu, L., et al. *Progressive Damage Detection/Diagnosis on Composite Using Electromechanical Impedance Spectroscopy*. in *Proceedings of the ASME International Mechanical Engineering Congress*. 2011. Denver, Colorado, USA.
8. Gresil, M., et al., *Predictive modeling of electromechanical impedance spectroscopy for composite materials.* Structural Health Monitoring, 2012. **11**(6): p. 671-683.
9. Gresil, M., et al., *Finite Element Modeling of Electromechanical Impedance for Damage Detection in Composite Materials.* 16th International Conference on Composite Structures, 2011.
10. Chandra, R., S.P. Singh, and K. Gupta, *Damping studies in fiber-reinforced composites - a review.* Composite Structures, 1999. **46**(1): p. 41-51.
11. Gibson, R.F., S.J. Hwang, and K. H. *Micromechanical modeling of damping in composite including interphase effects*. in *36th International SAMPE Symposium, Society for the Advancement of Material and Process Engineering*. 1991. Covina.
12. Nelson, D.H. and J.W. Hancock, *Interfacial slip and damping in fober reinforced composites.* J. Mater Sci, 1978. **13**: p. 2429-40.
13. Kenny, J.M. and M. Marchetti, *Elasto-plastic behavior of thermoplastic composite laminate under cyclic loading.* Composite Structures, 1995. **35**: p. 375-382.
14. Chaudhry, Z., et al. *Local-Area Health Monitoring of Aircraft via Piezoelectric Actuator/Sensor Patches*. in *Smart Structures and Integrated Systems SPIE*. 1995. SAn Diego, CA.
15. Liang, C., F.P. Sun, and C.A. Rogers, *Coupled Electro-Mechanical Analysis of Adaptive Material Systems â€" Determination of the Actuator Power Consumption and System Energy Transfer.* Journal of Intelligent Material Systems and Structures, 1994. **5**(1): p. 12-20.
16. Park, G., C. H.H, and I. D.J, *Impedance-based health moitoring of civil structural components.* ASCE Journal of Infrastructure Systems, 2000. **6**(4): p. 153-160.
17. Park, G., et al., *Overview of piezoelectric impedance-based Health Monitoring and Path Forward.* The Shock and Vibration Digest, 2003. **35**(6): p. 451-463.
18. Gresil, M. and V. Giurgiutiu. *Guided wave propagation in carbon composite laminate using piezoelectric wafer active sensors*. in *SPIE Smart Structures and Materials+ Nondestructive Evaluation and Health Monitoring*. 2013. San-Diego, CA, USA: International Society for Optics and Photonics.
19. Gresil, M. and V. Giurgiutiu, *Prediction of attenuated guided wave propagation in carbon fiber composites*, in *The 19th International Conference on Composite Materials*. 2013: Montreal, Canada.